

Excited-state relaxations and Franck-Condon shift in Si quantum dots

A. Franceschetti and S. T. Pantelides

Department of Physics, Vanderbilt University, Nashville, Tennessee 37235, USA

and Solid State Division, Oak Ridge National Laboratory, Oak Ridge, Tennessee 37831, USA

(Received 22 November 2002; revised manuscript received 4 March 2003; published 31 July 2003)

Excited-state relaxations in molecules are responsible for a redshift of the absorption peak with respect to the emission peak (Franck-Condon shift). The magnitude of this shift in semiconductor quantum dots is still unknown. Here we report first-principle calculations of excited-state relaxations in small (diameter ≤ 2.2 nm) Si nanocrystals, showing that the Franck-Condon shift is surprisingly large (~ 60 meV for a 2.2-nm-diameter nanocrystal). The physical mechanism responsible for the Stokes shift changes abruptly around ~ 1 nanometer in size, providing a clear demarcation between “molecules” and “nanocrystals.”

DOI: 10.1103/PhysRevB.68.033313

PACS number(s): 73.22.-f, 78.67.Bf

The Stokes shift commonly observed in molecules¹ and ionic solids² has its origin in excited-state atomic relaxations. When an electron-hole pair is created by optical excitation, the final state has approximately the same atomic configuration as the initial state (Franck-Condon principle). Prior to emission, however, the system can relax to a new configuration with lower total energy. Recombination occurs from the relaxed atomic configuration, leading to a redshift of the emission lines with respect to the absorption lines (Franck-Condon shift). The Franck-Condon shift in molecules can be as large as several eV. The magnitude of excited-state relaxations in semiconductor quantum dots, on the other hand, is still controversial. Quantum dots grown by colloidal chemistry methods range in size between 10^2 and 10^4 atoms, so excited-state relaxations could be significant. Continuum models based on elasticity theory, however, have predicted a Franck-Condon shift of only a few meV.^{3,4}

A schematic diagram of the relevant electronic energy levels as a function of the generic configuration variable \mathbf{R} is shown in Fig. 1. The minimum-energy atomic configuration of the quantum dot in the electronic ground state (GS) is different from the minimum-energy atomic configuration of the dot in the singlet (S) or triplet (T) excited states. At low temperature and in the absence of light, the quantum dot is in the ground-state geometry \mathbf{R}_{GS} . The lowest-energy allowed optical transition takes the system into the singlet excited state, as the lower-energy triplet state is optically inactive. Absorption can actually occur into several vibrational states associated with the singlet electronic state, leading to a broadening of the absorption line. The exciton relaxation then proceeds according to a few characteristic times: (i) spin-flip time τ_{flip} , which is the time required for the exciton to switch from the singlet state to the triplet state, (ii) recombination times $\tau_{rec}^{S,T}$ (with $\tau_{rec}^S \ll \tau_{rec}^T$), which include radiative and nonradiative recombination paths, and (iii) relaxation times $\tau_{rlx}^{S,T}$ in the singlet and triplet states, which are the characteristic times for the dissipation of the vibrational energy and are ultimately determined by the coupling of the quantum dot with the environment. If $\tau_{rlx}^{S,T} \ll \tau_{rec}^T$ (and $\tau_{flip} < \tau_{rec}^T$), the quantum dot relaxes to the lowest-energy triplet excited-state configuration (\mathbf{R}_{XS}) before the electron and the hole can recombine. In this case, the total Stokes shift is

$\Delta E = \Delta E_{FC} + \Delta E_{ST}$, where ΔE_{FC} is the Franck-Condon shift and ΔE_{ST} is the exciton exchange splitting. Different vibrational states may be involved in the emission process, leading to a broadening of the emission peak.^{1,2}

In this work, we investigate, using *ab initio* density-functional methods, the excited-state dynamics of Si quantum dots, and calculate the ensuing Franck-Condon shift. We find that in small Si quantum dots (1.0–2.2 nm diameter) the Franck-Condon shift is surprisingly large. For example, in the case of a ~ 2.2 -nm-diameter quantum dot we predict a Franck-Condon shift of ~ 60 meV, versus an exciton exchange splitting of only ~ 8 meV. By analyzing the physical mechanism responsible for the Franck-Condon shift we are able to identify two physically distinct regimes: for subnanometer Si clusters the dominant mechanism is the stretching of a single Si-Si bond upon electronic excitation, while for larger Si nanocrystals the Franck-Condon shift originates from a change in the overall shape of the nanocrystal in the presence of an electron-hole pair. This distinction provides a

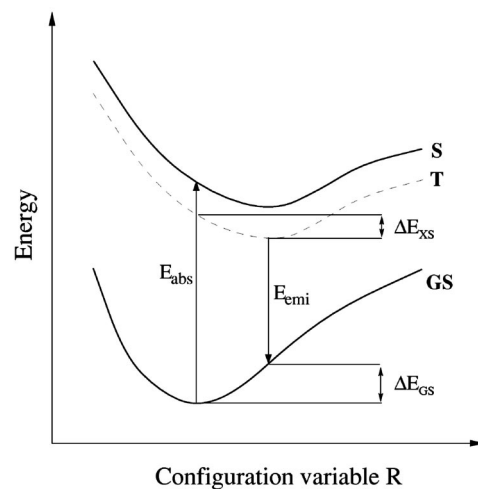


FIG. 1. Schematic diagram of the ground-state (GS) and excited-state singlet (S) and triplet (T) energy surfaces of a semiconductor quantum dot. Light is absorbed (E_{abs}) by exciting the quantum dot from the ground state to the optically active singlet state. Emission (E_{emi}) occurs from the triplet state, leading to a redshift of the emission line.

TABLE I. Calculated Franck-Condon shift ΔE_{FC} and electron-hole exchange splitting ΔE_{ST} (in eV) of hydrogen-passivated Si nanocrystals. Also shown are the ground-state and excited-state contributions to the Franck-Condon shift: $\Delta E_{FC} = \Delta E_{XS} + \Delta E_{GS}$. The absorption energy E_{abs} is estimated by adding the local spin-density band-gap error of bulk Si (0.7 eV) to the singlet excitation energy of the nanocrystal (see Ref. 15).

Nanocrystal	Diameter (Å)	E_{abs}	ΔE_{XS}	ΔE_{GS}	ΔE_{FC}	ΔE_{ST}
Si ₂₉ H ₃₆	10.3	4.3	0.79	2.13	2.92	0.051
Si ₈₇ H ₇₆	14.8	3.2	0.12	0.20	0.32	0.021
Si ₁₄₇ H ₁₀₀	17.6	2.8	0.09	0.12	0.21	0.014
Si ₂₇₅ H ₁₇₂	21.7	2.4	0.03	0.03	0.06	0.008

clear demarcation line between the molecular regime and the nanocrystal regime.

The calculations were performed using *ab initio* density-functional theory in the local spin-density (LSD) approximation. We used ultrasoft pseudopotentials to describe the electron-ion interaction, and the plane-wave representation (with an energy cutoff of 150 eV) to expand the Kohn-Sham orbitals. Triplet excited states can be calculated within density-functional theory by minimizing the total energy of the system in the triplet spin configuration (constrained density-functional approximation). We find that in practice, this approach works very well when compared with more sophisticated and computationally demanding techniques. For example, in the case of the silane molecule SiH₄, we calculate a triplet excitation energy of 8.1 eV. This should be compared with 8.5 eV obtained by solving the Bethe-Salpeter equation⁵ and 8.7 ± 0.1 eV obtained by quantum Monte Carlo simulations.⁵ In the limit of large quantum dots, we expect our approximation for the excitation energy to converge to the LSD band gap of bulk Si, which is ~ 0.7 eV smaller than the experimental band gap. Recent *ab initio* calculations of excited-state relaxations in molecules, using the Bethe-Salpeter formalism,⁶ have shown that the constrained density-functional approximation provides a very good estimate of the excited-state equilibrium geometry. Our approach to the calculation of excited states is applicable only to the lowest-energy triplet state, where the electron excited to the lowest unoccupied molecular orbital (LUMO) and the electron remaining in the highest occupied molecular orbital (HOMO) have parallel spin, i.e., $|T\rangle = |\uparrow\uparrow\rangle$. Calculations of the excited-state singlet energy surface would require the handling of a two-determinantal wave function, which is beyond the scope of simple density-functional theories (see, however, Ref. 7). For comparison, we have also performed excited-state calculations on the “mixed” energy surface given by $|M\rangle = |\uparrow\downarrow\rangle$. It can be shown that for a given atomic configuration, the energy difference $E^M - E^T$ is half of singlet-triplet splitting $E^S - E^T$ (see Ref. 7).

We consider here nearly spherical Si nanocrystals centered on a Si atom, having the T_d point-group symmetry in the ground-state geometry. The initial atomic configuration (before atomic relaxations) is obtained by cutting out a sphere from a bulk Si crystal. The Si-Si bond length is taken as the bulk LSD bond length (2.33 Å). The surface atoms having three dangling bonds are removed, while the remaining surface dangling bonds are passivated by H atoms. The

nanocrystals considered here range in size from 29 Si atoms (10.3 Å diameter) to 275 Si atoms (21.7 Å diameter).

The calculation of the Franck-Condon shift requires four steps.

(i) First, the ground-state atomic configuration is obtained by minimizing the total energy of the nanocrystal with respect to the atomic positions, as dictated by quantum-mechanical forces. This step gives the ground-state total energy $E^{GS}(\mathbf{R}_{GS})$.

(ii) Then we excite an electron-hole pair in the triplet state and calculate the excited-state energy in the ground-state geometry: $E^T(\mathbf{R}_{GS})$.

(iii) Next, we relax the atomic positions on the triplet excited-state energy surface, thus obtaining the excited-state total energy in the excited-state (XS) atomic configuration: $E^T(\mathbf{R}_{XS})$.

(iv) Finally, we calculate the ground-state total energy in the excited-state geometry $E^{GS}(\mathbf{R}_{XS})$.

The Franck-Condon shift ΔE_{FC} is then given by

$$\Delta E_{FC} = [E^T(\mathbf{R}_{GS}) - E^{GS}(\mathbf{R}_{GS})] - [E^T(\mathbf{R}_{XS}) - E^{GS}(\mathbf{R}_{XS})]. \quad (1)$$

ΔE_{FC} can be further decomposed into an excited-state contribution $\Delta E_{XS} = E^T(\mathbf{R}_{GS}) - E^T(\mathbf{R}_{XS})$ and a ground-state contribution $\Delta E_{GS} = E^{GS}(\mathbf{R}_{XS}) - E^{GS}(\mathbf{R}_{GS})$ (see Fig. 1). Note that ΔE_{XS} and ΔE_{GS} are total-energy differences between different atomic configurations of the same system. Thus, we expect the accuracy of the calculated Franck-Condon shift to be comparable with the accuracy of calculated vibrational energies (a few % error in the case of bulk Si).

The results for Si nanocrystals are summarized in Table I. Note that the ground-state contribution to the Franck-Condon shift ΔE_{GS} is larger than the excited-state contribution ΔE_{XS} , particularly for the smaller nanocrystals. This difference reflects the reduced curvature and increased nonparabolicity of the excited-state energy surface compared to the ground-state energy surface. Martin *et al.*³ proposed a simple model, based on the envelope-function approximation and empirical deformation potentials, to estimate the Franck-Condon shift in Si nanocrystal. They predicted that for a nanocrystal with an excitonic gap of 2.3 eV (approximately corresponding to the largest nanocrystal considered here) the Franck-Condon shift would range from 9 to 21 meV, depending on the parameters of the model. Using a similar con-

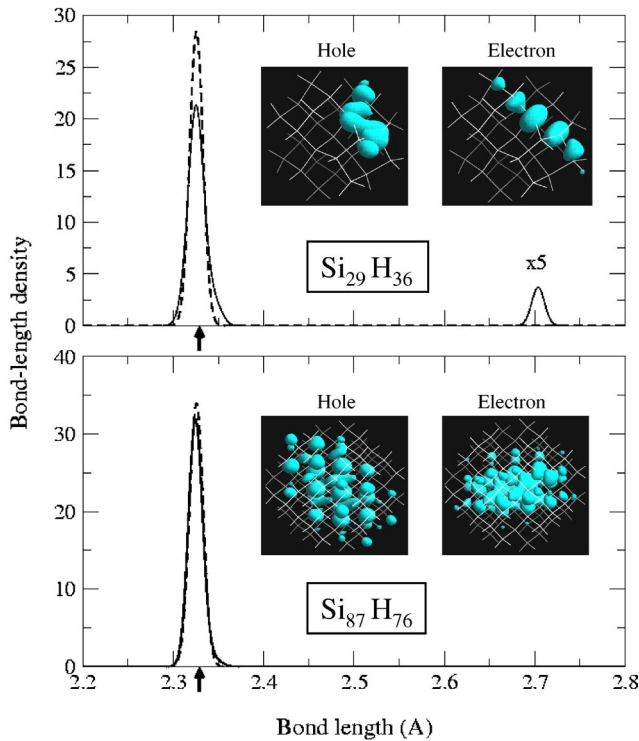


FIG. 2. Bond-length distribution in the ground-state geometry (dashed lines) and in the triplet excited-state geometry (solid lines) for the $\text{Si}_{29}\text{H}_{36}$ nanocrystal and the $\text{Si}_{87}\text{H}_{76}$ nanocrystal. The insets show the electron and hole single-particle wave functions in the excited-state configuration. The arrows denote the calculated bulk Si-Si bond length.

tinuum model, Takagahara and Takeda⁴ obtained a Stokes shift of ~ 7 meV for a nanocrystal of similar size. The approximations underlying these model calculations, namely, the effective-mass approximation and elasticity theory, are expected to break down in the limit of small nanocrystals, where the electron wave functions extend over a few interatomic distances. Our *ab initio* calculations show that these models significantly underestimate the Franck-Condon shift of small Si quantum dots.

The calculated Franck-Condon shift is very large in the small $\text{Si}_{29}\text{H}_{36}$ cluster, where the distortions due to the electronic excitation are large. Figure 2(a) shows the Si-Si bond-length distribution $n(L)$ of this cluster, both in the ground-state geometry and in the relaxed excited-state (triplet) geometry. We see that $n(L)$ is similar in the ground state and in the excited state, except for a single Si-Si bond in the interior of the nanocrystal that is stretched by about 15% in the excited-state geometry. The HOMO and LUMO wave functions in the excited-state geometry are strongly localized around the stretched Si-Si bond, as shown in the insets in Fig. 2(a), and the corresponding energy levels are well inside the band gap of the Si nanocrystal, thus producing the large Franck-Condon shift of 2.9 eV. Using tight-binding total-energy calculations, Allan, Deleure, and Lannoo⁸ predicted that in small hydrogen-passivated Si nanocrystals, excitons can become self-trapped in (meta)stable states localized at the surface. Our *ab initio* calculations show that excited-state

relaxations lead to the spontaneous formation of a stretched bond in the *interior* of the nanocrystal and therefore, the Franck-Condon shift should depend weakly on the type of surface passivation. Hirao⁹ calculated the Stokes shift of $\text{Si}_{29}\text{H}_{36}$ nanocrystals, finding a value of 0.22 eV, over an order of magnitude smaller than our result. This difference may be due to the lower energy cutoff used in the plane-wave expansion of Ref. 9.

Figure 2(b) shows the bond-length distribution of the $\text{Si}_{87}\text{H}_{76}$ nanocrystal. The distribution is centered around the bulk Si-Si bond length, with very little differences between the ground state and the excited state. In fact, we find that the Franck-Condon shift in this nanocrystal (and in larger nanocrystals) is due to a change in the overall shape of the nanocrystal, from spherical to ellipsoidal, upon electronic excitation. This change of shape leads to a splitting of the states at the top of the valence band (which are degenerate in the T_d representation) and thus, to the Franck-Condon shift. The insets in Fig. 2(b) show that the electron and hole wave functions in the excited-state configuration are delocalized over the entire nanocrystal.

As shown in Fig. 1, the exchange contribution to the Stokes shift is given (at low temperatures) by the singlet-triplet splitting ΔE_{ST} evaluated at the ground-state geometry \mathbf{R}_{GS} . We therefore calculate the exchange contribution as:

$$\Delta E_{ST} = 2[E^M(\mathbf{R}_{GS}) - E^T(\mathbf{R}_{GS})]. \quad (2)$$

The results are shown in the last column of Table I. We find that the electron-hole exchange splitting is significantly smaller than the Franck-Condon shift, even for the largest nanocrystal considered here. Spin-orbit coupling, which leads to a mixing of the triplet and singlet states, is small in Si, so it was not included in our calculations. Semiempirical pseudopotential calculations¹⁰ have shown that the effect of spin-orbit coupling is to reduce the electron-hole exchange splitting. The singlet-triplet splitting of Si nanocrystals had been calculated in the past using the effective-mass approximation,⁴ the tight-binding approximation,³ and the empirical pseudopotential method.¹¹ Our *ab initio* calculations are in good agreement with these calculations. For instance, for a Si nanocrystal with a predicted band gap of 2.4 eV, we find $\Delta E_{ST} = 8$ meV (see Table I). For nanocrystals with the same band gap, Martin *et al.*³ reported exchange splittings ranging from 6 to 12 meV, depending on the shape of the nanocrystal. Takagahara and Takeda⁴ and Reboredo, Franceschetti, and Zunger¹¹ found an exchange splitting of ~ 15 meV for spherical nanocrystals with a 2.4 eV band gap.

The Stokes shift of Si nanocrystals has been measured using both optical and thermal methods.^{12–14} Using selective laser excitation, Calcott *et al.*¹² and Kovalev *et al.*¹³ measured the redshift of the photoluminescence onset of Si nanocrystals with respect to the excitation energy. For example, for an excitation energy of 2.41 eV, Calcott *et al.*¹² reported a redshift of 23 meV. Similarly, Kovalev *et al.*¹³ measured a redshift of 12 meV for an excitation energy of 2.1 eV. The photoluminescence onset was attributed to zero-phonon emission, and the observed redshift was assigned

entirely to the electron-hole exchange splitting. The redshift was found to increase dramatically as the emission energy increases (or, alternatively, as the size of the nanocrystals decreases), as shown in Fig. 20 of Ref. 13.

Following the experimental work of Calcott *et al.*,¹² several semiempirical calculations of the electron-hole exchange splitting in Si nanocrystals have been reported in the literature,^{3,4,11} showing that the predicted exchange splitting is consistently smaller than the measured redshift. The difference can be as large as 50% in small Si nanocrystals. This discrepancy was attributed^{3,4} to the Franck-Condon shift. Model calculations based on elasticity theory⁴ indeed suggested that the Franck-Condon shift may account for the difference between the experimentally observed redshift and the calculated exchange splitting.

Based on our first-principles calculations, we note the following points:

(i) We confirm that the exchange splitting is smaller than the measured redshift. For example, for a 22 Å Si nanocrystal (with an estimated excitation energy of ~ 2.4 eV) we find an exchange splitting of only 8 meV (see Table I). This value should be compared with the 23 meV redshift observed in Si nanocrystals excited with a 2.4 eV laser light.¹²

(ii) The photoluminescence *onset* originates from zero-phonon emission, as pointed out in Ref. 12. Thus, the relevant Franck-Condon shift is ΔE_{XS} (see Fig. 1). For a 22-Å diameter Si nanocrystal we find $\Delta E_{XS} \approx 30$ meV (see Table

I), which is somewhat larger than the measured red shift of 23 meV.¹³

(iii) In the experiments of Refs. 12,13, a relatively large ensemble of nanocrystals are excited (namely, all the nanocrystals with an absorption feature at the excitation wavelength), but only a small set of nanocrystals contribute to the photoluminescence onset. Thus, the observed redshift is the minimum value of the redshift for the set of optically excited nanocrystals, as noted in Ref. 13. As a result, the measured redshift represents a lower bound for the red shift of hydrogen-passivated, nearly spherical Si nanocrystals, such as those considered in this work.

In conclusion, we have shown by excited-state density-functional calculations that the Franck-Condon shift in small Si nanocrystals is larger than previously thought. We have found that in subnanometer clusters, the Franck-Condon shift originates from the stretching of a Si-Si bond, while in larger nanocrystals it is due to a change in the overall shape of the nanocrystal upon electron-hole excitation.

This work was supported in part by the DOE Computational Materials Science Network Grant No. DE-FG02-02ER45972, NSF Grant No. DMR9803768, the US DOE under Contract No. DE-AC05-00OR22725 with the Oak Ridge National Laboratory, managed by UT-Battelle, LLC, and the William A. and Nancy F. McMinn Endowment at Vanderbilt University.

¹G. Herzberg, *Spectra of Diatomic Molecules* (Van Nostrand, New York, 1950).

²K.K. Rebane, *Impurity spectra of Solids; Elementary Theory of Vibrational Structure* (Plenum, New York, 1970).

³E. Martin *et al.*, Phys. Rev. B **50**, 18 258 (1994).

⁴T. Takagahara and K. Takeda, Phys. Rev. B **53**, R4 205 (1996).

⁵J.C. Grossman *et al.*, Phys. Rev. Lett. **86**, 472 (2001).

⁶S. Ismail-Beigi and S.G. Louie, Phys. Rev. Lett. **90**, 076401 (2003).

⁷I. Frank *et al.*, J. Chem. Phys. **108**, 4060 (1998).

⁸G. Allan, C. Delerue, and M. Lannoo, Phys. Rev. Lett. **76**, 2961 (1996).

⁹M. Hirao, in *Microcrystalline and Nanocrystalline Semiconductors*, edited by L. Brus, M. Hirose, R.W. Collins, F. Koch, and C.C. Tsai, Mater. Res. Soc. Symp. Proc. **358** (Materials Research Society, Pittsburgh, 1995).

¹⁰A. Franceschetti, L.W. Wang, H. Fu, and A. Zunger, Phys. Rev. B **58**, R13 367 (1998).

¹¹F.A. Rebrodo, A. Franceschetti, and A. Zunger, Phys. Rev. B **61**, 13 073 (2000); Appl. Phys. Lett. **75**, 2972 (1999).

¹²P.D.J. Calcott *et al.*, J. Phys.: Condens. Matter **5**, L91 (1993).

¹³D. Kovalev *et al.*, Phys. Status Solidi B **215**, 871 (1998).

¹⁴M.L. Brongersma *et al.*, Appl. Phys. Lett. **76**, 351 (2000).

¹⁵C. Delerue, M. Lannoo, and G. Allan, Phys. Rev. Lett. **84**, 2457 (2000).